Scattering Delay Network: an Interactive Reverberator for Computer Games

Enzo De Sena[1], Hüseyin Hacıhabiboğlu[1,2], and Zoran Cvetković[1]

[1]*Centre for Telecommunications Research, Department of Informatics, King's College London, WC1R 2LS, London, UK*

[2]*Department of Modeling and Simulation, Informatics Institute, METU, Ankara, 06531, Turkey*

Correspondence should be addressed to Enzo De Sena (`enzo.desena@kcl.ac.uk`)

ABSTRACT

Many 3D computer games incorporate audio renderers simulating room acoustics to provide the user with a high level of immersiveness and realism. Full-scale interactive room auralisation systems are impractical for use in computer games due to their high computational cost. As a low-cost alternative, artificial reverberators can be used. This paper is concerned with the design of a scalable interactive reverberator inspired by digital waveguide mesh (DWM) models and feedback delay networks (FDN). This reverberator is by construction tightly linked to the acoustics of the enclosure that it simulates. Simulation of unequal and frequency-dependent wall absorption, as well as directional sources and microphones can also be incorporated. It is shown that the response of the proposed reverberator accurately renders the early reflections and room modes, as well as providing RT60 values consistent with Sabine and Eyring equations.

1. INTRODUCTION

A typical user of computer games usually enjoys spatial audio through a stereophonic setup or a multichannel system. Audio signals to be played back are usually generated by an audio renderer using the properties of the modelled acoustic space and the enclosed sound sources, as well as the position of the user within the simulated virtual environment. Interactive room auralisation systems which allow auditory navigation, and context awareness within virtual environments can be used for this purpose. An interactive room auralisation system requires real-time operation as well as independent control of parameters such as listener and source positions [1]. There have been attempts to use image-source model [2], beam tracing [3], and ray tracing [4] to interactively simulate room acoustics. Similarly, numerical models such as digital waveguide meshes (DWM) can be used to simulate room acoustics [5, 6, 7]. Although these models provide very accurate results, they suffer from high computational and memory requirements making them impractical in interactive applications such as computer games. Advent of graphical processing units which incorporates many cores started to make real-time numerical models a possibility at least on high-end platforms [8]. However, even on computer games run on high-end hardware, priority is given to graphics when allocating resources. Therefore, using a lightweight audio renderer is preferable.

Articial reverberators present a good alternative to full-scale room simulation. A popular articial reverberator is the feedback delay network (FDN) [9] which provides high quality reverberation with a low computational complexity. FDN reverberators are suitable for real-time operation even on hardware with modest computational capabilities such as mobile phones, tablet PCs, or portable game consoles. FDN reverberators consist of several absorptive delay lines cross-connected over a unitary feedback delay matrix in the feedback path. The mathematical equivalence of FDN reverberators with DWM models has previously been shown [10]. This equivalence stems from the fact that both FDN reverberators and DWM models use unitary matrices, and that FDN reverberators can be considered as a special case of DWM models with a single scattering junction [10]. This equivalence, together with perceptual models of distance perception, was exploited in the design of a reverberator capable of panning source distance [11].

This paper is concerned with the design of a scalable reverberator model that can be used in interactive computer games and virtual reality applications. The proposed design is based on the use of scattering nodes located on

the walls of the modelled volume and interconnected by bidirectional delay lines. These scattering nodes are connected to one or more source signal injection nodes and one or more microphone nodes via absorptive unidirectional delay lines. In addition, the source nodes are connected to microphone nodes over attenuating unidirectional delay lines to simulate direct sound propagation path. Source and microphone directivity can also be simulated to obtain more realistic virtual recordings in the simulated room. A similar approach to artificial reverberation was first proposed by Smith [12] and investigated further by Karjalainen *et al.* in [13]. The similarities and differences of the proposed reverberator with that approach will also be highlighted.

The paper is organised as follows. Sec. 2 presents a brief overview of FDN reverberators and DWM models and highlights the similarities between these two models. Sec. 3 presents the scattering delay network (SDN) approach proposed in this paper. The transfer function of the reverberator is derived in Sec. 3.3. Sec. 4.1 presents a numerical evaluation of the SDN reverberator. Sec. 5 concludes the paper.

2. BACKGROUND

2.1. Digital Waveguide Mesh Models

Digital waveguide meshes (DWM) are simple numerical models that can be used to solve wave equation in acoustic media [14]. DWM models involve sampling of the domain whose acoustics is to be modelled. Each sample in the DWM model is represented by an *N*-port scattering junction, connected to its geometric neighbours over bidirectional delay lines. Execution of a DWM model involves two successive stages at each iteration: the *scattering pass*, and the *propagation step*. The solution of the wave equation is obtained during the scattering pass by a simple matrix operation and the obtained solution is propagated in the model at the propagation stage. In order to demonstrate this operation let us consider the interconnected DWM junctions shown in Fig. 1.

At a given iteration, n, the outgoing wave variables $\mathbf{p}_i^-(n)$ at junction i are obtained from incoming wave variables $\mathbf{p}_i^+(n)$ by the scattering pass which involves the matrix multiplication:

$$\mathbf{p}_i^-(n) = \mathbf{S}\mathbf{p}_i^+(n) \qquad (1)$$
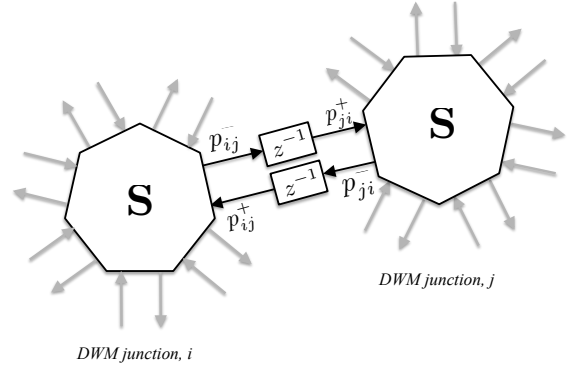
Fig. 1: Two interconnected DWM junctions, i and j, with scattering matrix $\mathbf{S}$. Incoming and outgoing wave variables are denoted and p_{ij}^+, p_{ij}^-, p_{ji}^+, and p_{ji}^-, respectively.

where

$$\mathbf{p}_i^+(n) = \begin{bmatrix} p_{i1}^+(n) & \cdots & p_{ij}^+(n) & \cdots & p_{iN}^+(n) \end{bmatrix}^T,$$

$$\mathbf{p}_i^-(n) = \begin{bmatrix} p_{i1}^-(n) & \cdots & p_{ij}^-(n) & \cdots & p_{iN}^-(n) \end{bmatrix}^T,$$

$$\mathbf{S} = \frac{2}{N}\mathbf{1}_{NxN} - \mathbf{I},$$

are the incoming and outgoing wave variable vectors, and the scattering matrix, respectively. This operation is called the *scattering pass*. The calculated outgoing wave variables are then propagated throughout the model by the bidirectional delay lines such that $p_{ij}^+(n+1) = p_{ji}^-(n)$. This step is called the *propagation step*. These two steps allow the calculation of the response at each point in the modelled acoustical system.

Room acoustics can be modelled with two [15] or three [16] dimensional DWM models. The associated computational load is prohibitively high for real-time operation. Advances in multicore graphical processing units (GPUs) made fast implementations of DWMs possible [8]. However, DWMs are still confined to high-end systems with specialized hardware and require a considerable amount of memory.

2.2. Feedback Delay Networks

Feedback delay networks (FDN) were first proposed by Stautner and Puckette as a multichannel generalisation of recursive reverberators [18]. The original model was based on a so-called 'lossless' prototype which used a
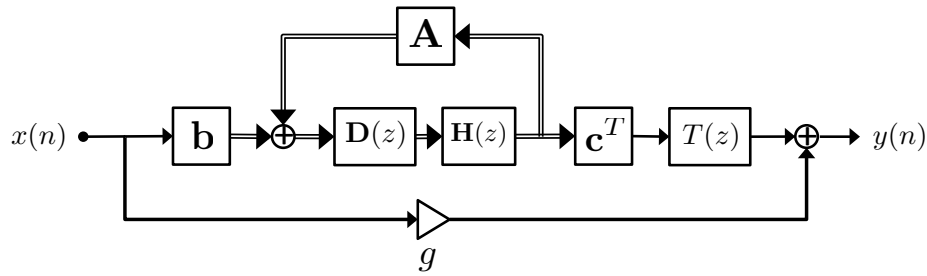
Fig. 2: Block diagram of the modified FDN reverberator as proposed by Jot and Chaigne [17].

unitary feedback matrix, $\mathbf{A}$ (i.e.$\mathbf{A}\mathbf{A}^T = \mathbf{I}$) in the feedback path connected onto itself by delay lines in the feedforward path. This way, N reverberated signals could be obtained from N independent inputs to be played back over an N-channel audio system or mixed to obtain any desired number of channels. The feedback matrix is not unique and can be selected to be any unitary matrix, but with varying results [19]. For example if the $N \times N$ feedback matrix $\mathbf{A} = \mathbf{I}$ the FDN structure can be simplified to N comb filters connected in parallel and acts as the Schroeder reverberator [20].

Jot and Chaigne proposed an improved version of FDN reverberators by including absorbent filters on each feedforward path as well as a *tone correction filter* [17]. Here, $\mathbf{A}$ is the unitary feedback matrix, b_i is the input gain, c_i is the output gain, m_i is the integer delay, and $H_i(z)$ is the absorbent filter associated with channel i, and $T(z)$ is the tone correction filter. It is possible using this reverberator to control the modal decay characteristics of the reverberant time, but in an indirect way. The transfer function of this reverberator can be expressed as:

$$Y(z) = T(z)\mathbf{c}^T \mathbf{q}(z) + gX(z), \tag{2}$$
$$\mathbf{q}(z) = \mathbf{H}(z)\mathbf{D}(z)[\mathbf{A}\mathbf{q}(z) + \mathbf{b}X(z)]. \tag{3}$$

Here,
$$\mathbf{q}(z) = [s_1(z)\ s_2(z)\ \cdots\ s_N(z)]^T$$

is the state vector,
$$\mathbf{b} = [b_1\ b_2\ \cdots\ b_N]^T,$$
$$\mathbf{c} = [c_1\ c_2\ \cdots\ c_N]^T,$$

are the gain vectors,
$$\mathbf{H}(z) = \mathrm{diag}(H_1(z),\ H_2(z),\ \cdots,\ H_N(z)),$$

is the absorptive filter matrix,

$$\mathbf{D}(z) = \mathrm{diag}(z^{-m_1},\ z^{-m_2},\ \cdots,\ z^{-m_N}),$$

is the delay matrix, $\mathbf{A}$ is a unitary feedback matrix, and g is the gain of the direct path. The frequency response of this multichannel system can be expressed as:

$$H(z) = \frac{Y(z)}{X(z)} = T(z)\mathbf{c}^T[\mathbf{H}(z^{-1})\mathbf{D}(z^{-1}) - \mathbf{A}]^{-1}\mathbf{b} + g. \tag{4}$$

Fig. 2 shows the block diagram of this reverberator.

An interesting aspect of FDN-type reverberators is their similarity with DWM models [10]. Namely, each DWM junction is a special case of an FDN reverberator, making a multidimensional DWM a network of interconnected FDN reverberators. This similarity manifests itself in the fact that both DWM junctions and FDN-type reverberators carry out a scattering operation with unitary matrices. In the case of a densely sampled DWM, the actual solution of the wave equation is obtained. In the case of an FDN reverberator, the reverberation characteristics of a room is emulated without any consideration of physical accuracy. This similarity was previously exploited to obtain a simple two-channel reverberator [11].

3. SCATTERING DELAY NETWORKS

3.1. Design overview
The artificial reverberator proposed in this paper uses one scattering node for each wall of the modelled enclosure. These node are connected to each other via bidirectional, absorptive delay lines. In addition, a source injection node and a microphone node are connected to the scattering nodes by unidirectional attenuating delay lines. The direct path is modelled by the connection between the
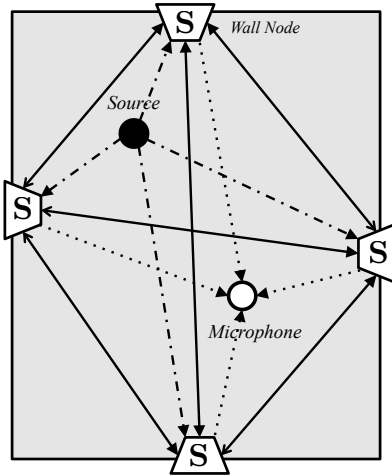
Fig. 3: Proposed SDN reverberator with interconnected wall nodes, source injection node and the microphone node (2D case).

source injection node and the microphone node. Due to the nature of the operations carried out to obtain reverberation, we call this reverberator as the *scattering delay network* (SDN) reverberator and the scattering nodes as SDN nodes. There are four types of connections in the proposed model. These are the connections between SDN nodes, source node and SDN nodes, SDN nodes and microphone node, and source node and microphone node. Fig. 3 shows a conceptual depiction of the SDN reverberator.

3.1.1. **SDN nodes**
Each SDN node is positioned on a wall of the modelled enclosure and is connected to other nodes by absorptive bidirectional delay lines. These nodes carry out a scattering operation on their inputs from other nodes to obtain the outputs. This scattering operation is carried out using a unitary (i.e. energy preserving) scattering matrix. For a room with N walls, the number of neighbours that a SDN node has is $N-1$. The scattering matrix employed in this paper is the DWN scattering matrix:

$$\mathbf{S} = \frac{2}{N-1}\mathbf{1}_{(N-1)\times(N-1)} - \mathbf{I}, \qquad (5)$$

which is common to all the SDN nodes in the reverberator. While results presented in this paper were obtained with (5), other unitary matrix could be used as well. The pressure at the SDN node is a combination of incoming wave variables, $p_{ki}^+(n)$, from neighbouring nodes and
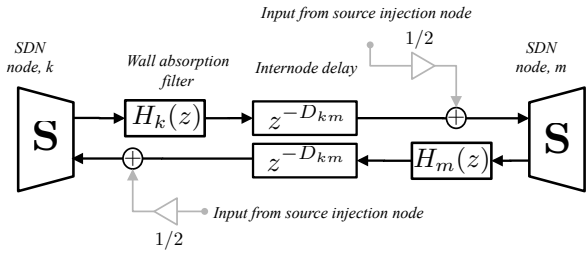
Fig. 4: Two interconnected SDN nodes.

the pressure, $p_{Sk}(n)$, due to the source as observed at the node:

$$p_k(n) = p_{Sk}(n) + \frac{2}{N-1}\sum_{i=1}^{N-1} p_{ki}^+(n). \qquad (6)$$

In order to simplify the calculation, input from source can be distributed to incoming wave variables such that:

$$\tilde{p}_{ki}^+(n) = p_{ki}^+(n) + 0.5\, p_{Sk}(n), \qquad (7)$$

which provides the intended node pressure.

3.1.2. **SDN interconnections**
The connections between the SDN nodes consist of a bidirectional delay element modelling the propagation path delay, and two absorption filters which models the wall absorption associated with the two interconnected nodes. These interconnections due to their recirculating nature are responsible for the modelling of the room reverberation by facilitating the simulation of energy exchange between walls. The connection between two SDN nodes is depicted in Fig. 4.

The length of the delay lines connecting these individual nodes is determined by the actual positions of the nodes. These positions are calculated so as to provide first-order early reflections having the correct delay and the correct angle of incidence at a microphone position at $\mathbf{x}_M$ for a source positioned at $\mathbf{x}_S$. This can be done by calculating the point at which a *sound ray* emitted from the sound source and received at the microphone hits the wall. This calculation is trivial for simple geometries such as shoebox enclosures.

For a volume with N walls, the number of bidirectional inter-node connections is $\binom{N}{2}$. The length of the integer delay line between the k-th and m-th node is calculated as $D_{km} = \lfloor F_s\|\mathbf{x}_k - \mathbf{x}_m\|/c\rfloor$, where c is the speed of sound, F_s is the sampling rate, and $\mathbf{x}_i$ is the position vector of the i-th SDN node.
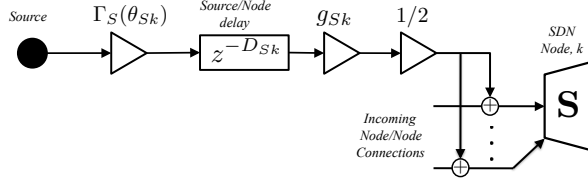
Fig. 5: Connection between the source node and a SDN node.

The losses due to wall absorption can be incorporated into the model via filters, $H_k(z)$ and $H_m(z)$ modelling the absorptive properties of the walls, k and m, respectively. These can be selected as minimum-phase IIR filters in order to reduce computational load without affecting the phase response of the simulated reflection [21].

3.1.3. Source to SDN connections

The input to the system from an individual source is provided by a source injection node connected to SDN nodes via unidirectional attenuating delay lines (see Fig. 5).

The length of the delay line between the source at $\mathbf{x}_S$ and the SDN node positioned at $\mathbf{x}_k$ is determined by the propagation delay $D_{Sk} = \lfloor F_s \|\mathbf{x}_S - \mathbf{x}_k\|/c \rfloor$. As there is no backscattering to the source node or spreading of energy by the source node in the proposed model, the attenuation due to spherical spreading ($1/r$ law) should also be incorporated into this delay line as

$$g_{Sk} = \frac{G}{\|\mathbf{x}_S - \mathbf{x}_k\|}, \tag{8}$$

where G is the unit-distance in the model, i.e. c/F_s, where F_s is the sampling frequency.

Another important simulation parameter is the source directivity. The sparse sampling of the simulated enclosure prohibits the simulation of source directivity in great detail. However, a coarse approximation is easily incorporated by weighting the outgoing signals by $\Gamma_S(\theta_{Sk})$, where $\Gamma_S(\theta)$ is the source directivity, and θ_{Sk} is the angle formed between the source reference axis and the line connecting source and k-th node. The pressure at the SDN node due to the source is then:

$$p_{Sk}(n) = g_{Sk}\Gamma_S(\theta_{Sk})p_S(n - D_{Sk}). \tag{9}$$

This value is input to an SDN node by first scaling it with $1/2$ and adding it to each incoming internode connection to the SDN node, as explained in equation (7).
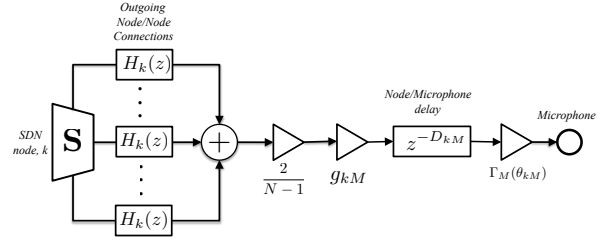
Fig. 6: Connection between an SDN node and the microphone node.

3.1.4. SDN to microphone connections

The connection between the SDN node and the microphone node consists of a unidirectional attenuating delay line (see Fig. 6). The input signal is taken as the summation of the outgoing pressure variables at the node (after passing through the wall filters) multiplied by $2/(N-1)$. The delay from the k-th SDN node to the microphone node is $D_{kM} = \lfloor F_s \|\mathbf{x}_k - \mathbf{x}_M\|/c \rfloor$. As with source directivity, the microphone directivity is also modelled using a simple gain element. The attenuation on the delay line is set as:

$$g_{kM} = \frac{1}{1 + \frac{\|\mathbf{x}_k - \mathbf{x}_M\|}{\|\mathbf{x}_S - \mathbf{x}_k\|}}, \tag{10}$$

such that

$$g_{Sk}g_{Mk} = \frac{G}{\|\mathbf{x}_S - \mathbf{x}_k\| + \|\mathbf{x}_k - \mathbf{x}_M\|}, \tag{11}$$

which yields the correct attenuation for the first order reflection according to $1/r$ law.

3.2. Scalability and interactivity

The proposed method is scalable to different audio reproduction formats. For coincident microphone formats (e.g. Ambisonics), only the microphone gains $\Gamma_{Mk}(\theta)$ have to be adjusted. For the setups involving spatially separated microphones, one SDN reverberator have to be employed for each microphone. For near-coincident microphone setups, the same SDN node structure can be used, while creating new, dedicated node-to-microphone delay lines for each microphone, at the cost of reducing the accuracy of the system slightly. It is also possible to obtain approximate virtual binaural recordings. For this, a pair of head related transfer function filters (HRTF) for each SDN node and source injection node needs to be used.
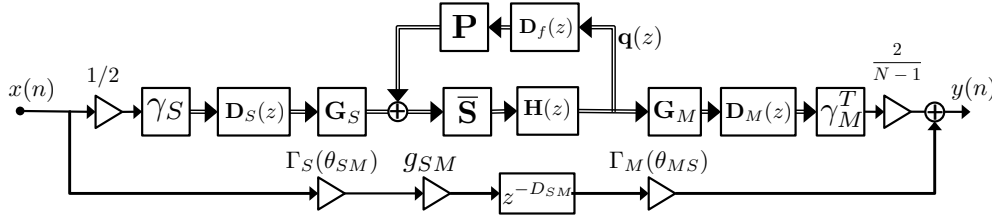
Fig. 7: The block diagram of the SDN reverberator.

The SDN reverberator also allows interactive operation. This is done via updating the model to reflect changes in the positions and rotations of source and the microphone. This requires adjusting the positions of the nodes, and updating the delay line lengths and gains accordingly.

3.3. Transfer function of the SDN reverberator

While the SDN reverberator is inspired by the combination of DWM models and FDN reverberators its overall structure is different. Fig. 7 shows the simplified block diagram of the SDN reverberator. In the figure,

$$\boldsymbol{\gamma}_S = [\underbrace{\Gamma_S(\theta_{S1})\cdots\Gamma_S(\theta_{S1})}_{N-1}\Gamma_S(\theta_{S2}) \cdots \Gamma_S(\theta_{SN})]^T$$

$$\boldsymbol{\gamma}_M = [\underbrace{\Gamma_M(\theta_{1M})\cdots\Gamma_M(\theta_{1M})}_{N-1}\Gamma_M(\theta_{2M}) \cdots \Gamma_M(\theta_{NM})]^T$$

are the $N(N-1) \times 1$ source and microphone directivity vectors,

$$\mathbf{D}_S(z) = \mathrm{diag}(\underbrace{z^{-D_{S1}}\cdots z^{-D_{S1}}}_{N-1}, z^{-D_{S2}} \cdots z^{-D_{SN}})$$

$$\mathbf{D}_M(z) = \mathrm{diag}(\underbrace{z^{-D_{M1}}\cdots z^{-D_{M1}}}_{N-1}, z^{-D_{M2}} \cdots z^{-D_{MN}})$$

are $N(N-1) \times N(N-1)$ source and microphone delay matrices,

$$\mathbf{G}_S = \mathrm{diag}(\underbrace{g_{S1}\cdots g_{S1}}_{N-1}, g_{S2}\cdots g_{SN})$$

$$\mathbf{G}_M = \mathrm{diag}(\underbrace{g_{M1}\cdots g_{M1}}_{N-1}, g_{M2}\cdots g_{MN})$$

are the source and microphone attenuation matrices,

$$\overline{\mathbf{S}} = \mathrm{diag}(\underbrace{\mathbf{S}, \mathbf{S}, \cdots, \mathbf{S}}_{N})$$

is a $N(N-1) \times N(N-1)$ (unitary) block diagonal matrix representing the overall scattering operation with $\mathbf{S} = \frac{2}{N-1}\mathbf{1}_{N-1\times N-1} - \mathbf{I}$,

$$\mathbf{D}_f(z) = \mathrm{diag}(z^{-D_{12}}, \cdots, z^{-D_{NN-1}})$$

is the $N(N-1) \times N(N-1)$ delay matrix representing the internode delays,

$$\mathbf{H}(z) = \mathrm{diag}(\underbrace{H_1(z)\cdots H_1(z)}_{N-1}, H_2(z)\cdots H_N(z))$$

is the $N(N-1) \times N(N-1)$ wall absorption matrix, $\mathbf{P}$ is a permutation matrix whose elements are determined based on adjacency of SDN nodes, g_{SM} is the direct path attenuation from source to microphone, and $z^{-D_{SM}}$ is the direct path delay.

From inspection of Fig. 7 the system output can be expressed as:

$$y = \frac{2}{N-1}\boldsymbol{\gamma}_M^T \mathbf{D}_M \mathbf{G}_M \mathbf{q} + \overline{g}z^{-D_{SM}} \qquad (12)$$

where $\overline{g} = g_{SM}\Gamma_S(\theta_{SM})\Gamma_M(\theta_{MS})$, and $\mathbf{q}$ is the state vector, which is given by

$$\mathbf{q} = \mathbf{H}\overline{\mathbf{S}}\left(\mathbf{PD}_f\mathbf{q} + \tfrac{1}{2}\mathbf{G}_S\mathbf{D}_S\boldsymbol{\gamma}_S x\right) \qquad (13)$$

$$= \tfrac{1}{2}\left(\mathbf{I} - \mathbf{H}\overline{\mathbf{S}}\mathbf{PD}_f\right)^{-1}\mathbf{H}\overline{\mathbf{S}}\mathbf{G}_S\mathbf{D}_S\boldsymbol{\gamma}_S x \qquad (14)$$

The transfer function of SDN reverberators can therefore be expressed as:

$$H(z) = \overline{g}z^{-D_{SM}} + \tfrac{1}{N-1}\mathbf{k}_M(z)\left(\mathbf{H}(z^{-1}) - \overline{\mathbf{S}}\mathbf{PD}_f(z)\right)^{-1}\overline{\mathbf{S}}\mathbf{k}_S(z),$$
$$\qquad (15)$$

where $\mathbf{k}_M = \boldsymbol{\gamma}_M^T \mathbf{D}_M \mathbf{G}_M$ and $\mathbf{k}_S = \mathbf{G}_S\mathbf{D}_S\boldsymbol{\gamma}_S$.

It may be observed that unlike FDN-type reverberators different acoustical aspects such as the direct path and reflection delays are clearly delineated so as to allow a

direct correspondence to the acoustics of the modelled room and complete flexibility with respect to source and microphone positions and directivities. In addition, the inclusion of first-order reflections directly into the model makes using a separate early-reflection module unnecessary.

3.4. Relation to previous work

An artificial reverberator using a similar sparse network of scattering nodes was also proposed by Smith [12], and further developed by Karjalainen *et al.* [13]. While this reverberator, which we will refer to as DWN reverberator, has similarities with the SDN reverberator proposed in this paper, there are also significant differences:

1. In the DWN reverberator, the microphone node is itself a scattering node connected to the sparse DWM network, whereas the microphone node in the SDN reverberator is a passive element, which is actually the case for a real microphone.

2. In the DWN reverberator, additional waveguides co-directional with the room axes are connected to the microphone node, and these nodes are interconnected with some of the other scattering nodes. While accuracy of axial frequency modes is improved by this, it also increases the computational complexity.

3. The absorptive losses are modelled by loading the DWN wall nodes with frequency-dependent admittance via self connections. It was reported that in order to control reverberation time and improve naturalness, these admittance loads have to be tuned heuristically. The SDN nodes do not have self connections and absorptive losses are modelled by short, minimum-phase IIR filters on the bidirectional delay lines. This allows incorporation of wall materials with known absorption coefficients directly.

4. In the DWN reverberator, only source-to-node and source-to-microphone attenuations were included. This causes inaccuracies in the magnitudes of the first-order reflections, particularly when the source is close to one of the wall nodes. This problem was circumvented by adding separate delay lines from source to microphone according to the image source principle. SDN reverberators do not suffer from the same problem, as they are able to render first order reflections correctly.

4. NUMERICAL EVALUATION

In the first part of this section, several room impulse responses (RIR) generated by SDN reverberators are shown, along with their energy decay curves. An evaluation of the decay rate and the associated reverberation time T_{60} is then carried out, followed by an analysis of the acoustical frequency modes generated by the proposed reverberator. Finally, an evaluation of the impact of frequency-dependent wall absorption on the reverberation time is given.

4.1. Examples

The RIR of a shoebox room with dimensions $\mathbf{l} = [l_x, l_y, l_z] = [9, 7, 4]$ is shown in Fig. 8. Having defined the reference system origin in one of the room vertices, the source was placed at the centre of the room $\mathbf{x}_s = [4.5, 3.5, 2]$, and the microphone at $\mathbf{x}_s = [2, 2, 1.5]$. The model was run with different wall absorption coefficients. In Fig. 8(a) all the walls have the frequency-independent absorption coefficient $\alpha = 0.2$, which corresponds to wall filters of the kind $H_i(z) = \beta = \sqrt{1 - \alpha} = 0.89$, where β is the reflection coefficient. It may be observed in Fig. 8 that both attenuation and delay of first order reflections are correctly rendered by the model. In Fig. 8(b), a slightly higher absorption coefficient of $\alpha = 0.3$ is employed. As expected, a similar response to the case $\alpha = 0.2$ is obtained, but with a faster decay.

Actual rooms have walls with different absorption characteristics (brick wall, carpet, ceiling...), which are also frequency dependent. Fig. 8(c) shows a more realistic example, where absorption filters $H_i(z)$ modelling these surfaces are employed. Each filter was implemented as a minimum-phase IIR filter. The filter coefficients were optimised through damped Gauss-Newton method to fit the absorption coefficients reported by Vorländer in [22]. Second or third order filters were used, which provided an acceptable residual error with low computational requirements. The floor covering was modelled as *cotton carpet*, while for the ceiling *fissured ceiling tiles* were used. The model for the side walls was *average hard surface*.

In Fig. 9 the energy decay curves (EDC) are shown for the three examples given above. For the two cases with uniform walls, the decay is consistently exponential, while for the more realistic case with frequency dependent absorption, a non-exponential decay is observed.
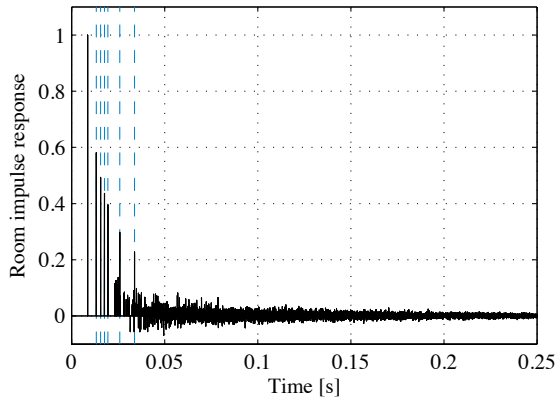
(a) Uniform walls with frequency independent absorption $\alpha = 0.2$
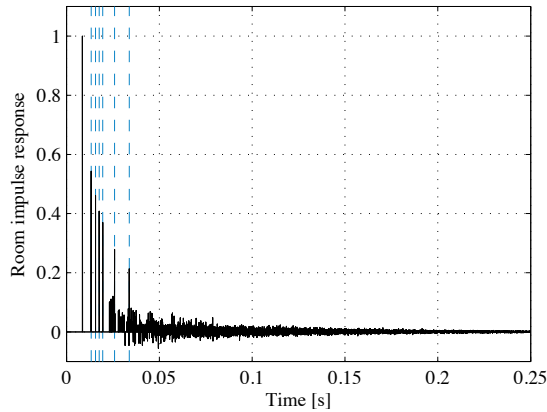
(b) Uniform walls with frequency independent absorption $\alpha = 0.3$
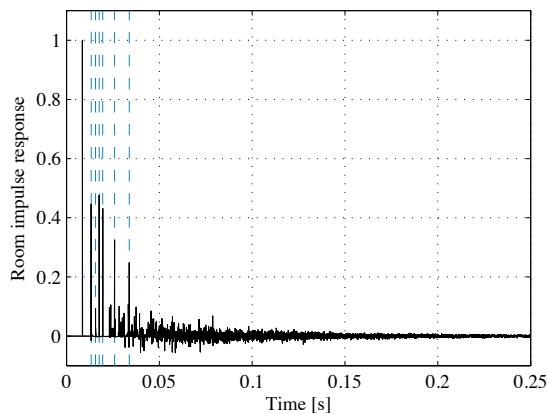
(c) Walls with realistic frequency-dependent absorption (cement walls, cotton carpet, fissured ceiling tiles)

Fig. 8: Examples of different room impulse responses. The vertical lines indicate the actual delay of the first order reflections.
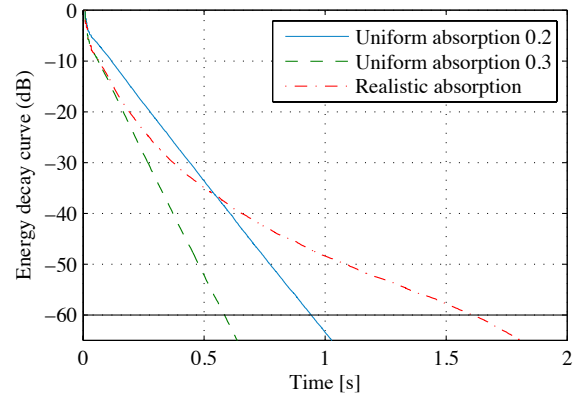
Fig. 9: Energy decay curves of the room impulse response in Fig 8.

4.2. Reverberation time

As a rough metric to assess the performance of the proposed method, the reverberation time predicted by the two well-known formulas according to Sabine [23] and Eyring [24] are considered:

$$T_{60,Sab} = \frac{0.161V}{\sum_i A_i \alpha_i} \qquad (16)$$

$$T_{60,Eyr} = -\frac{0.161V}{(\sum_i A_i) \log_{10}(1 - \sum_i A_i \alpha_i / \sum_i A_i)} \qquad (17)$$

where $V = l_x \cdot l_y \cdot l_z$ is the room volume, A_i and α_i are the area and absorption coefficient of the i-th wall, respectively. For the examples with frequency independent absorption presented in Sec. 4.1, the calculated reverberation time is $T_{60} = 0.94$ for $\alpha = 0.2$, and $T_{60} = 0.58$, for $\alpha = 0.3$. These values are close to the reverberation time predicted by Sabine formula. In fact $T_{60,Sab} = 0.80$ for $\alpha = 0.2$, and $T_{60,Sab} = 0.53$ for $\alpha = 0.3$.

As a more general assessment of the reverberation time rendered by the proposed model, cubic rooms with uniform and frequency independent absorption were simulated. The ISO recommendation [25] suggests a minimum distance between source and microphone for the measurement of reverberation time. This distance is given by:

$$d_{min} = 2\sqrt{\frac{V}{cT_{est}}} \qquad (18)$$

where T_{est} is a rough estimation of the reverberation time. Observe that (18) is a function of the room size. Moreover, for small enclosures, the value of (18) can be bigger than the room itself, and, in this case, it is suggested

(a) $\alpha = 0.3$ (b) $\alpha = 0.6$ (c) $\alpha = 0.9$
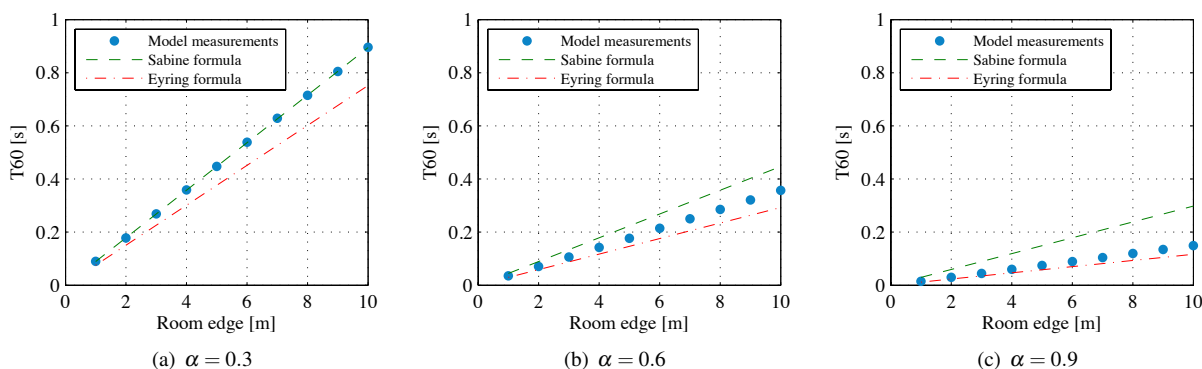
Fig. 10: Values of reverberation time T60 with different absorption coefficients α.

[25] that the line-of-sight component should be removed. To avoid changing the experimental conditions when the size of the room is changed, source and microphone were both placed in the middle of the room. The line-of-sight component was removed in all cases before calculating T_{60}.

In Fig. 10, the results are shown for three different absorption coefficients $\alpha = 0.3, 0.6, 0.9$, and cubic rooms $\mathbf{l} = [r, r, r]$, with edge lengths $r = 1, ..., 10$ m. As a first remark, the proposed model generates RIR with reverberation times that increase linearly with r. This is in agreement with both Sabine and Eyring formulas, which, in this simplified case, reduce to:

$$T_{60,Sab} = \frac{0.161r}{6\alpha},$$

$$T_{60,Eyr} = -\frac{0.161r}{6\log_{10}(1-\alpha)}.$$

Moreover, for $\alpha = 0.3$ the calculated T_{60} are very close to the predictions of Sabine formula. It is well known that Sabine formula tends to overestimate reverberation time for high absorptive materials [24]. As absorption gets higher (see Fig. 10(b) and 10(c)), the reverberation time decreases at a greater rate than Sabine's formula, supporting the fact that the proposed method produces consistent energy decay rates. Finally, the calculated T_{60} values get closer to Eyring's formula (which provides better approximation in rooms with more absorptive walls) as α increases.

4.3. Low frequency room modes

One of the main acoustical properties of a room is given by its frequency modes, i.e. the frequencies that yield

resonance phenomena in the room. For a shoebox enclosure, these acoustical modes are given by [23]:

$$f_{n_x,n_y,n_z} = \frac{c}{2}\sqrt{\left(\frac{n_x}{l_x}\right)^2 + \left(\frac{n_y}{l_y}\right)^2 + \left(\frac{n_z}{l_z}\right)^2} \quad (19)$$

where $n_x, n_y, n_z = 0, 1, ..., +\infty$. Accurate room simulation models should render such frequency modes in the form of peaks and dips (depending on the position of source and microphone) in the room frequency response. In Fig. 11 it is shown that the proposed SDN reverberator exhibits this interesting feature, as most of the axial modes (i.e. $f_{n_x,0,0}$, $f_{0,n_y,0}$, and $f_{0,0,n_z}$) correspond to critical points in the low-frequency response. This example was run using a room with dimensions $\mathbf{l} = [2, 2.14, 3.74]$.
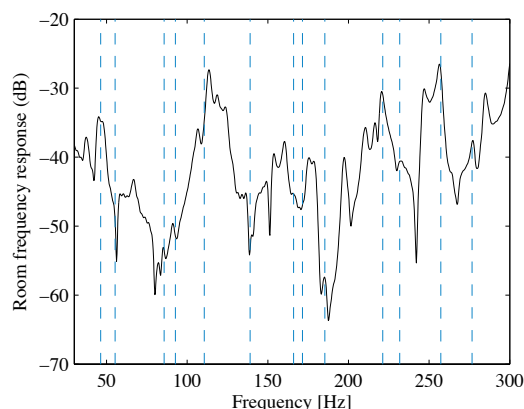
Fig. 11: Frequency response of the simulated room. The highlighted vertical lines indicate the axial frequency modes of the room.
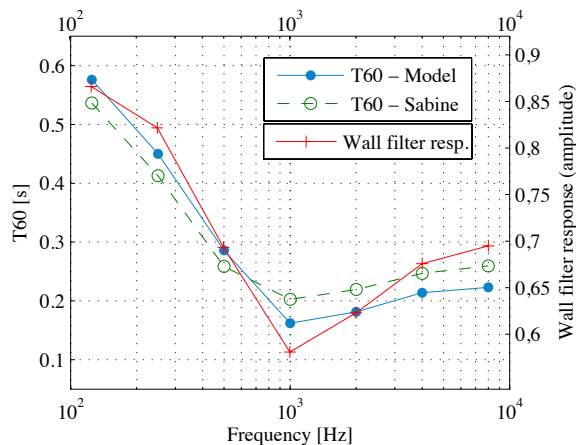
Fig. 12: Relation between the wall frequency response and the reverberation time in different octave bands. Note the two different y-axis: the left axis relates to Sabine's and calculated T_{60}, while the right axis refers to the amplitude of the wall filter response.

The source and microphone were positioned on the axis connecting the two opposite vertices and 1 m away from one another around the centre of the room. In order to highlight the modes, the absorption coefficient was set to the relatively low value of $\alpha = 0.12$.

4.4. Frequency-dependent reverberation

It is discussed below that the reverberation time provided by the model in different octave bands follows the magnitude response characteristics of the wall absorption filter.

Among the realistic materials employed previously, *cotton carpet* was selected for all the walls. The employed filter $H(z)$ was the same IIR minimum-phase filter used in Sec. 4.1. Source and microphone were positioned on the axis connecting the two opposite vertices of a cubic room $\mathbf{l} = [5,5,5]$. They were positioned around the centre of the room, at a distance given by (18), where the T_{est} was chosen using Sabine formula, which yielded $d_{min} = 2.96$.

In Fig. 12 results of this simulation are shown. The wall filter response is plotted, together with the corresponding Sabine predictions, obtained as:

$$T_{60,Sab} = \frac{0.161V}{\sum_i A_i \alpha_i(\omega)} = \frac{0.161 \cdot 5}{6\alpha(\omega)} = \frac{0.161 \cdot 5}{6(1 - |H(e^{j\omega})|^2)}$$

The simulated RIR was fed into an octave-band filter bank, and T_{60} values were calculated for each octave-

band. As shown in Fig. 12, these measured T_{60} are very close to Sabine's formula prediction, thus confirming that the proposed model allows for explicit control of wall properties.

Furthermore, in case direct control of reverberation time is preferred, the prediction functions (16) or (17) can be inverted to obtain $\alpha(\omega)$, and appropriate wall filters can be designed to fit $\alpha(\omega)$. To this end, Eyring's formula (17) is preferable [24], as (16) is known to yield non-physical values $\alpha > 1$ for some acoustically "dead" rooms.

5. CONCLUSIONS

This paper presented a scalable and interactive reverberator capable of simulating the acoustics of a virtual room. The room is modelled by scattering nodes interconnected by bidirectional delay lines. These scattering nodes are positioned at the points where first-order reflections originate. This way, the first-order reflections are simulated correctly, while a rich but less accurate reverberation tail is obtained. The transfer function of the system was derived, and examples were given to demonstrate its performance. Informal listening tests showed that SDN reverberator provided natural sounding reverberation without artifacts.

6. REFERENCES

[1] L. Savioja, J. Huopaniemi, T. Lokki, and R. Väänänen, "Creating interactive virtual acoustic environments," *J. Audio Eng. Soc.*, vol. 47, no. 9, pp. 675–705, 1999.

[2] J. Huopaniemi, *Virtual Acoustics and 3-D Sound in Multimedia Signal Processing*, Ph.D. thesis, Helsinki University of Technology, Espoo, Finland, 1999.

[3] T. Funkhouser, N. Tsingos, I Calborn, G. Elko, M. Sondhi, J.E. West, G. Pingali, P Min, and A. Ngan, "A beam tracing method for interactive architectural acoustics," *J. Acoust. Soc. Am.*, vol. 115, no. 2, pp. 739–756, 2004.

[4] M. Taylor, A. Chandak, L. Antani, and D. Manocha, "Resound: Interactive sound rendering for dynamic virtual environments," in *Proc. 17th Int. ACM Conf. on Multimedia*, 271-280, Ed., Beijing, China, October 19-24 2009.

[5] D. T. Murphy and D. M. Howard, "Modelling and directionally encoding the acoustics of a room," *Elect. Lett.*, vol. 34, no. 9, pp. 864–865, April 1998.

[6] S. A. Van Duyne and J. O. Smith, III, "The tetrahedral digital waveguide mesh," in *Proc. of 1995 IEEE Workshop on Appl. of Signal Process. to Audio and Acoust. (WASPAA'95)*, New Paltz, NY, USA, 15-18 October 1995, pp. 234–237.

[7] L. Savioja and V. Valimaki, "Interpolated rectangular 3-D digital waveguide mesh algorithms with frequency warping," *IEEE Trans. on Speech and Audio Process.*, vol. 11, no. 6, pp. 783–790, 2004.

[8] L. Savioja, "Real-time 3D finite-difference time-domain simulation of low- and mid-frequency room acoustics," in *Proc. 13th Int. Conf. on Digital Audio Effects (DAFx-10)*, September 2010.

[9] W. G. Gardner, "Reverberation algorithms," in *Applications of Digital Signal Processing to Audio and Acoustics*, M Kahrs and K Brandenburg, Eds., Boston, MA, USA, 1998, pp. 85–131, Kluwer Academic.

[10] D. Rocchesso, "Circulant and elliptic feedback delay networks for artificial reverberation," *IEEE Trans. on Speech and Audio Process.*, vol. 5, no. 1, pp. 51–63, January 1997.

[11] S. Mate-Cid, H. Hacıhabiboğlu, and Z. Cvetković, "Stereophonic rendering of source distance using dwm-fdn artificial reverberators," in *Proc. 128th Conv. of the Audio Eng. Soc., Preprint #8030*, London, UK, 22-25 May 2010.

[12] J. O. Smith, III, "A new approach to digital reverberation using closed waveguide networks," in *Proc. 11th Int. Comput. Music Conf.*, Burnaby, BC, Canada, 1985, pp. 47–53.

[13] M. Karjalainen, P. Huang, and J.O. Smith, "Digital Waveguide Networks for Room Response Modeling and Synthesis," in *Proc. 118th Conv. Audio Eng. Soc., Preprint # 6394*, Barcelona, Spain, 2005.

[14] S. D. Bilbao, *Wave and scattering methods for numerical simulation*, Wiley, 2004.

[15] A. Kelloniemi, V. Valimaki, and L. Savioja, "Simulation of room acoustics using 2-D digital waveguide meshes," in *Proc. of IEEE Int. Conf. Acoust., Speech and Signal Process. (ICASSP), 2006*. IEEE, 2006, vol. 5.

[16] H. Hacıhabiboğlu, B. Günel, and Z. Cvetković, "Simulation of directional microphones in digital waveguide mesh-based models of room acoustics," *IEEE Trans. on Audio, Speech and Language Process.*, vol. 18, no. 2, pp. 213–223, February 2010.

[17] J-M. Jot and A Chaigne, "Digital delay networks for designing artificial reverberators," in *Proc. 104th Conv. Audio Eng. Soc., Preprint # 3030*, Paris, France, 1991.

[18] J. Stautner and M. Puckette, "Designing multichannel reverberators," *Computer Music J.*, vol. 6, no. 1, pp. 52–65, 1982.

[19] C. Faller and F. Menzer, "Unitary Matrix Design for Diffuse Jot Reverberators," in *Proc. 128th Conv. Audio Eng. Soc. , Preprint # 7984*, London, UK, 2010.

[20] M. R. Schroeder, "Natural-sounding artificial reverberation," *J. Audio Eng. Soc.*, vol. 10, no. 3, pp. 219–233, 1962.

[21] J. Huopaniemi, L. Savioja, and M. Karjalainen, "Modeling of reflections and air absorption in acoustical spaces a digital filter design approach," in *Proc. 1997 IEEE Workshop on Appl. of Signal Process. to Audio and Acoust. (WASPAA'97)*, New Paltz, NY, USA, October 19-22 1997.

[22] M. Vorlander, *Auralization: fundamentals of acoustics, modelling, simulation, algorithms and acoustic virtual reality*, Springer Verlag, 2008.

[23] H. Kuttruff, *Room Acoustics*, SPON Press, London, UK, 4th edition, 2000.

[24] C. F. Eyring, "Reverberation time in "dead" rooms," *J. Acoust. Soc. Am.*, vol. 1, pp. 168, 1930.

[25] International Standards Organization, "3382. Acoustics–Measurement of the reverberation time of rooms with reference to other acoustical parameters," 1997.